

See discussions, stats, and author profiles for this publication at: <https://www.researchgate.net/publication/227705311>

Comparison of straight chain and cyclic unnatural amino acids embedded in the core of staphylococcal nuclease

ARTICLE *in* PROTEIN SCIENCE · AUGUST 1997

Impact Factor: 2.85 · DOI: 10.1002/pro.5560060803 · Source: PubMed

CITATIONS

14

READS

31

4 AUTHORS, INCLUDING:



[Robert O. Fox](#)

University of Houston

67 PUBLICATIONS 3,448 CITATIONS

[SEE PROFILE](#)

Comparison of straight chain and cyclic unnatural amino acids embedded in the core of staphylococcal nuclease

RICHARD WYNN,^{1,3} PAUL C. HARKINS,^{1,2,4} FREDERIC M. RICHARDS,¹
AND ROBERT O. FOX^{1,2,5}

¹Department of Molecular Biophysics and Biochemistry, Yale University, New Haven, Connecticut 06511

²Howard Hughes Medical Institute, Yale University, New Haven, Connecticut 06511

(RECEIVED February 14, 1997; ACCEPTED April 30, 1997)

Abstract

We have determined by X-ray crystallography the structures of several variants of staphylococcal nuclease with long flexible straight chain and equivalent length cyclic unnatural amino acid side chains embedded in the protein core. The terminal atoms in the straight side chains are not well defined by the observed electron density even though they remain buried within the protein interior. We have previously observed this behavior and have suggested that it may arise from the addition of side-chain vibrational and oscillational motions with each bond as a side chain grows away from the relatively rigid protein main chain and/or the population of multiple rotamers (Wynn R, Harkins P, Richards FM, Fox RO. 1996. Mobile unnatural amino acid side chains in the core of staphylococcal nuclease. *Protein Sci* 5:1026–1031). Reduction of the number of degrees of freedom by cyclization of a side chain would be expected to constrain these motions. These side chains are in fact well defined in the structures described here. Over-packing of the protein core results in a 1.0 Å shift of helix 1 away from the site of mutation. Additionally, we have determined the structure of a side chain containing a single hydrogen to fluorine atom replacement on a methyl group. A fluorine atom is intermediate in size between methyl group and a hydrogen atom. The fluorine atom is observed in a single position indicating it does not rotate like methyl hydrogen atoms. This change also causes subtle differences in the packing interactions.

Keywords: protein dynamics; protein folding; protein structure; unnatural amino acids

Quantitative assessment of the forces that drive protein folding and binding processes remains one of the most fundamental problems challenging physical biochemists today. Protein interiors are tightly packed (Richards, 1977) with little cavity volume (Hubbard et al., 1994). Steric complementarity provides many favorable Van der Waals contacts but how this affects the core dynamics is not precisely known. These motions may be related to longer time-scale motions that are necessary for folding and/or biological activity. The relationship between tight packing and dynamics will also have a thermodynamic consequence in terms of the vibrational entropy of the system (Doig & Sternberg, 1995).

Reprint requests to: Richard Wynn, Dupont Merck Pharmaceutical Co., Experimental Station, E336/241B, P.O. Box 80336, Wilmington, DE 19880; e-mail: wynn@al.lldmpc.umc.dupont.com.

³Present address: The Dupont Merck Pharmaceutical Co., Experimental Station, E336/241B, P.O. Box 80336, Wilmington, Delaware 19880.

⁴Present address: Department of Biochemistry, University of Texas Southwestern Medical Center, Dallas, Texas.

⁵Present address: Department of Human Biological Chemistry and Genetics, University of Texas, Medical Branch at Galveston, and Sealy Center for Structural Biology, Galveston, Texas 77555-0647.

Abbreviations: BME, β-mercaptopropanoic acid; cC5, cyclopentane; cC6, cyclohexane; FE, 2-fluoroethane; pdTp, 3',5' thymidine diphosphate; RMSD, root mean square deviation; SA, simulated annealing.

Previously, we have introduced long linear unnatural amino acid side chains into position 23 of staphylococcal nuclease (Wynn et al., 1995, 1996). This work relies on a combined mutagenesis/chemical modification method (Wynn & Richards, 1993), which uses chemical modification of a cysteine residue buried in the native structure after denaturant induced unfolding. The resultant side chains contain disulfide bonds to a variety of hydrocarbon moieties. We will refer to a protein variant by the thiol that forms a disulfide with Cys23 of the protein, i.e., the variant with a cyclopentane cysteine disulfide will be referred to as the cyclopentane variant. The thermodynamic stability (Wynn et al., 1995) and native state structures (Wynn et al., 1996) for a series of variants containing methyl, ethyl, 1-n-propyl, 1-n-butyl, and 1-n-pentyl disulfides have been determined. When examined by X-ray crystallography, the terminal atoms in the longest of these side chains were not well defined by the observed electron density, indicating greater thermal motion than is normally observed for buried residues in proteins. We have concluded that tight packing in a protein core in the absence of strong covalent constraints does not significantly damp the vibrational and oscillational motions of an amino acid side chain as it extends from the relatively rigid main chain. The motion amplitude would increase with distance from the main-chain “anchor” as multiple bond motions become engaged—this behavior is not likely to be observed for the relatively short natural

amino acid side chains. Here we report the structures of several variants with even longer side chains (1-n-hexyl and 1-n-heptyl) and cyclic side chains (cyclopentane and cyclohexane) and compare the behavior of equivalent length straight chains and cyclic side chains. Additionally, we report the structure of a fluoroethane variant and compare it with structures containing the similar side chains of ethane, propane, and 2-hydroxyethyl disulfides.

Results and discussion

The structure of staphylococcal nuclease consists of a six-stranded antiparallel β -barrel (Fig. 1A, shown in blue) and three α -helices (Fig. 1A, shown in green). Position 23, the site of mutation in this study, lies in the third strand and its side chain is directed toward the center of the β -barrel. It is surrounded by residues Leu14, Leu25, Phe34, Leu36, Thr62, Val66, Ile72, Ile92, and Val99 (Fig. 1B, using a 4.0 Å cutoff). Helix 1, which will be discussed further below, is comprised of residues 54–68 and packs into the β -barrel. In the structure of wild-type staphylococcal nuclease-pdTp-Ca²⁺ complex, no electron density is observed for residues 1 to 6 and 142 to 149 (Loll & Lattman, 1989). We also do not observe any electron density for these residues in the structures reported in this work.

Large hydrophobic side chains

Global structural change

There is no large global structural change for any of the variants in this study. The RMSDs from the unmodified cysteine variant vary from 0.26 Å (n-heptyl) to 0.30 Å (cyclohexyl). Additionally, all variants have activities towards p-nitrophenyl substrates similar to the wild-type protein (data not shown). Previously we have reported that introduction of a large hydrophobic side chain such as a 1-n-pentyl cysteine disulfide side chain at position 23 results in a 1.0 Å displacement of helix 1 away from the main body of the β -barrel due to close contacts between position 23 and Val66 (Wynn

et al., 1996). The structures of the 1-n-hexyl, 1-n-heptyl, cyclopentane, and cyclohexane variants show very similar displacements. As with the 1-n-pentyl variant, residues 54–66 keep main-chain dihedral angles and hydrogen-bonding patterns characteristic of α -helices in all of these structures; the structural response is a rigid body movement. This result is striking in that this perturbation of the native structure parallels the character of a nuclease kinetic intermediate characterized by hydrogen exchange measurements (Jacobs & Fox, 1994). These experiments showed the largest protection in the β -barrel region and very little protection in helix 1. Our structures show that when the β -barrel region is over-packed, most of the structural change results in a displacement of the helix and the β -barrel geometry is largely maintained.

Packing of interior residues

The packing around the 1-n-hexyl, 1-n-heptyl, cyclopentane, and cyclohexane side chains remains largely unchanged from that observed in the unmodified cysteine variant structure. No rotamer changes, relative to the wild-type protein structure, take place with the exception of a rotamer flip about χ_1 for Thr62 in the cyclohexane structure. The residues surrounding position 23 are held in place by extensive secondary interactions; these side chains retain the wild-type conformations when position 23 varies from two (cysteine) to 10 (1-n-heptyl) non-hydrogen atoms in a linear chain from the α -carbon. This lack of rotameric changes suggests that the Van der Waal interactions in wild-type nuclease have been maximized to a particular steric fit. Space for the hydrocarbon moieties is created by the movement of helix 1 away from the β -barrel (discussed above)—no contacts shorter than 3.3 Å between the hydrocarbon moieties of the hexane and heptane variants are observed. If the 1-n-hexane moiety is removed from the structure, a cavity of 218 Å³ results. This volume is close to that expected for a group of this size.

The displacement of helix 1 away from the β -barrel in the pentyl variant results in formation of a cavity of 29 Å³ in the space between the two secondary structural elements (Wynn et al., 1996).

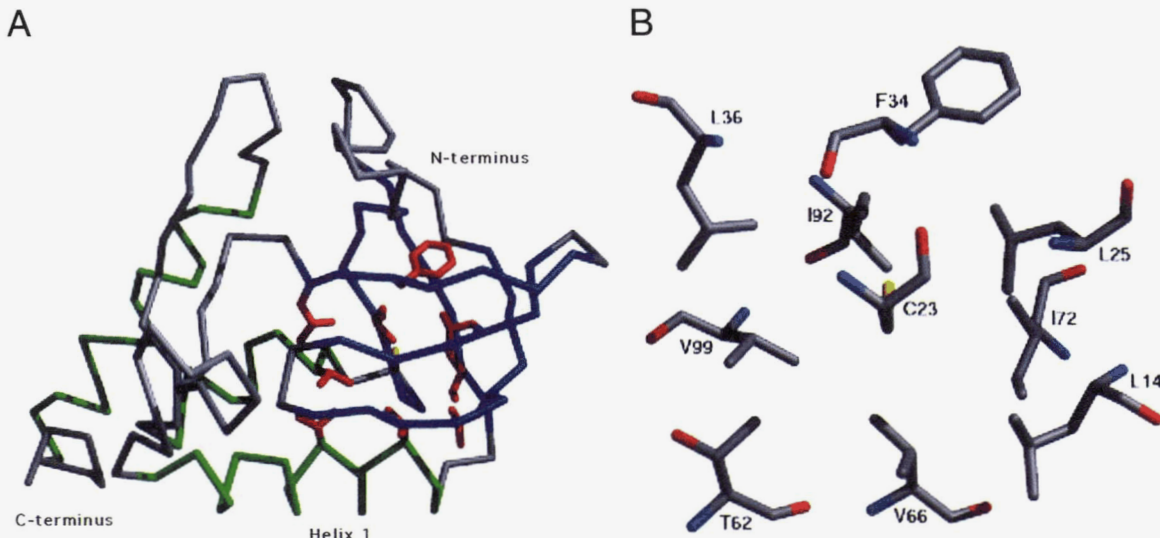


Fig. 1. **A:** C α trace of staphylococcal nuclease. Segments are color coded according to secondary structure: Blue, β -sheet; green α -helix. The side chains of Cys23 and surrounding residues are shown. **B:** Close-up of the amino acids that surround residue 23. Residues are labeled next to the α -carbon and color coded according to atom type. The orientation from the left panel is preserved.

The butyl variant has a smaller cavity of 17 \AA^3 . In the hexyl variant this cavity is not observed because the third and fourth carbon atoms of the hexyl side chain protrude into this cavity space. The heptyl variant once again shows a small cavity of 17 \AA^3 . It is surrounded by residues Val66, Thr72, Ile92, Val99, and the hydrocarbon chain of residue 23. The cyclopentyl and cyclohexyl variants also show small cavities in this region (both are 19 \AA^3). Thus, complete space filling relies on a subtle interplay among side-chain volume, shape, and flexibility.

Protein dynamics

The most striking observation in our previous work was the absence of electron density for the terminal atoms in the longer side chains. These long side chains may undergo increased thermal motion relative to the surrounding side chains with motion increasing further out from the relatively rigid main chain, a conclusion that is tentatively supported by molecular dynamics calculations (Wynn et al., 1996). However, alternative rotamers not sampled during our molecular dynamics calculations cannot be ruled out. This electron density pattern is once again observed for the longer linear hydrocarbon side chains studied here. Figure 2 (top half) shows $(F_o - F_c)$ omit maps for position 23 for the 1-n-pentyl, 1-n-hexyl, and 1-n-heptyl side chains. The motion observed increases for atoms further out from the main chain in a pattern very similar to that observed in lipid bilayers (Rance et al., 1980). The surrounding residues are well defined by the observed electron density and do not show increased *B*-factors relative to the wild type or unmodified V23C protein structure.

The anchoring of a side-chain terminus by a non-covalent interaction could potentially decrease the motion observed. In fact, when a β -hydroxyl ethyl side chain was introduced at position 23, the terminal hydroxyl group formed a hydrogen bond to the carbonyl oxygen of residue 19 and this resulted in substantially decreased motion, relative to the isosteric propyl side chain, as indicated by the observed electron density and *B* factors for position 23 (Wynn et al., 1996). The addition of covalent constraints, as in the cyclopentane and cyclohexane moieties, should have a similar effect on protein dynamics. Figure 2 (bottom half) shows $(F_o - F_c)$ omit maps for these variants. These side chains are clearly delineated by the observed electron density. There is also a significant decrease in the observed *B*-factors upon cyclization of the hexane side chain—*B*-factors range from 60 to 80 \AA^2 in the straight chain variant and 37 to 48 \AA^2 in the cyclic variant. The *B*-factors of the hydrocarbon moiety for the pentane and cyclopentane variant average 45 \AA^2 and 46 \AA^2 respectively. The lack of *B*-factor change in this instance may result from a combination of the unusual pseudorotation dynamics of cyclopentane rings (Cui et al., 1993) and the overall higher *B*-factors for the cyclopentane structure (mean side-chain *B*-factors of 32.5 \AA^2 and 35.2 \AA^2 , respectively). The additional conformational constraints imposed upon the side chain by cyclization appear to decrease the motion these groups undergo relative to the equivalent length linear side chains. In this case, the damping of motion through cyclization is apparently larger than any similar effect that might be caused due to tight packing in the protein interior. Previously, MD simulations have shown little vibrational entropy loss due to packing in the native state (Karplus et al., 1987). Recent NMR results also sup-

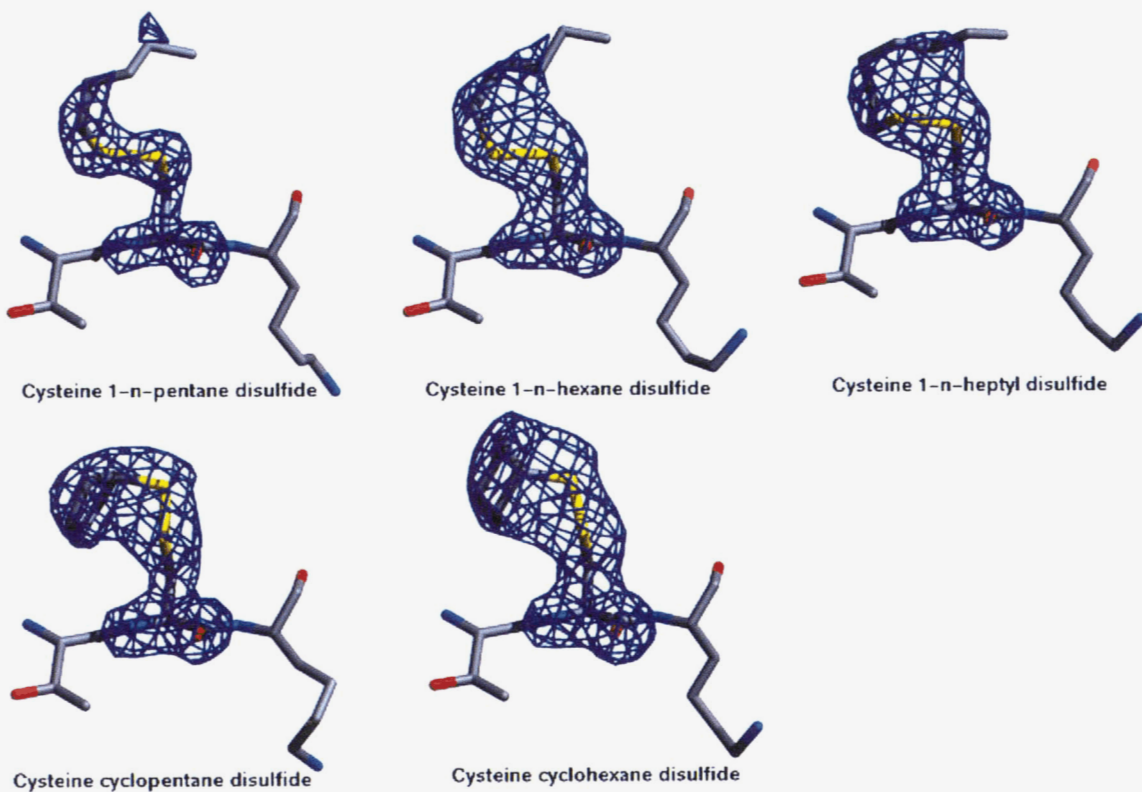


Fig. 2. $(F_o - F_c)$ position 23 omit maps contoured at 3.5σ . Maps were calculated in XPLOR (Brünger, 1992) and displayed using the program MIDAS (Computer Graphics Laboratory, University of California, San Francisco).

port this notion (Wand et al., 1996). Packing is not optimized to these unnatural amino acids. A well-defined core with long linear chains could potentially be realized through the optimization of packing interactions. It is possible to bind long chain hydrocarbons in well-defined conformations as is the case with fatty acid binding protein-fatty acid complexes (reviewed by Banaszak et al., 1994). It should be noted that Sacchettini et al. (1989) have observed an increase in *B*-factors in the carbons of palmitate bound to rat intestinal fatty acid binding protein as the distance from the carboxylate group increases.

Cyclic side-chain rotamers

An important characteristic of protein structure is that side chains packed in the protein interior almost always populate a well known distribution of "rotamers," which is dictated by the torsional angle potentials for the dihedrals involved (Ponder & Richards, 1987). While we cannot definitively rule out other conformations based on the observed electron density, the cyclic side chains studied here seem to follow the same behavior. The cyclohexane ring refines to the well known chair conformation in our structure and the cyclopentane ring adopts an envelope conformation that is favored for five-membered rings (Fuchs, 1978). The fact that side-chain dihedral angles almost always fall in an energy minimum suggests that packing of a protein interior does not overcome the torsional angle constraints of these groups. This would also suggest that packing may not have a large effect on the dynamic behavior of the protein interior.

Fluoroethane structure

The 2-fluoroethane side chain is similar to the ethyl, 1-propyl, and BME side chains we have previously studied and involves only hydrogen to fluorine, methyl to fluorine, and hydroxyl to fluorine changes, respectively. The fact that fluorine is intermediate in size between a hydrogen and a methyl (or hydroxyl) group offers a very minimal change, which could not be reproduced among natural amino acids. Will the small size of a fluorine group lower the barriers to rotation so that a single conformation would not be observed? Similarly, if free rotation did not occur, would the fluorine atom populate three positions nearly equally as rotation would switch a hydrogen for a comparably sized fluorine atom? Figure 3 (top) shows ($F_o - F_c$) maps for both position 23 (blue) and the fluorine atom (green). Clearly, only a single position is populated by the fluorine atom. The fluorine atom makes contact (<4.0 Å) with the C, C α , and N of Thr22, and the C γ and C β of Leu36.

The ethyl, propyl, and BME structures do not show any cavities and we have previously speculated that the volumes of these side chains approach the volume limit position 23 can tolerate without significant structural change (Wynn et al., 1996). The fluoroethane structure also does not show any cavities. However, the protein interior apparently discriminates between these very similar side chains. In the propyl variant, close contact between the propyl group and Ile92 causes rotation of C δ of Ile92 away from position 23. This behavior is not observed in the ethyl variant (Fig. 3, bottom panel, left half). In the BME variant a hydrogen bond between the side-chain hydroxyl group of residue 23 and the main-

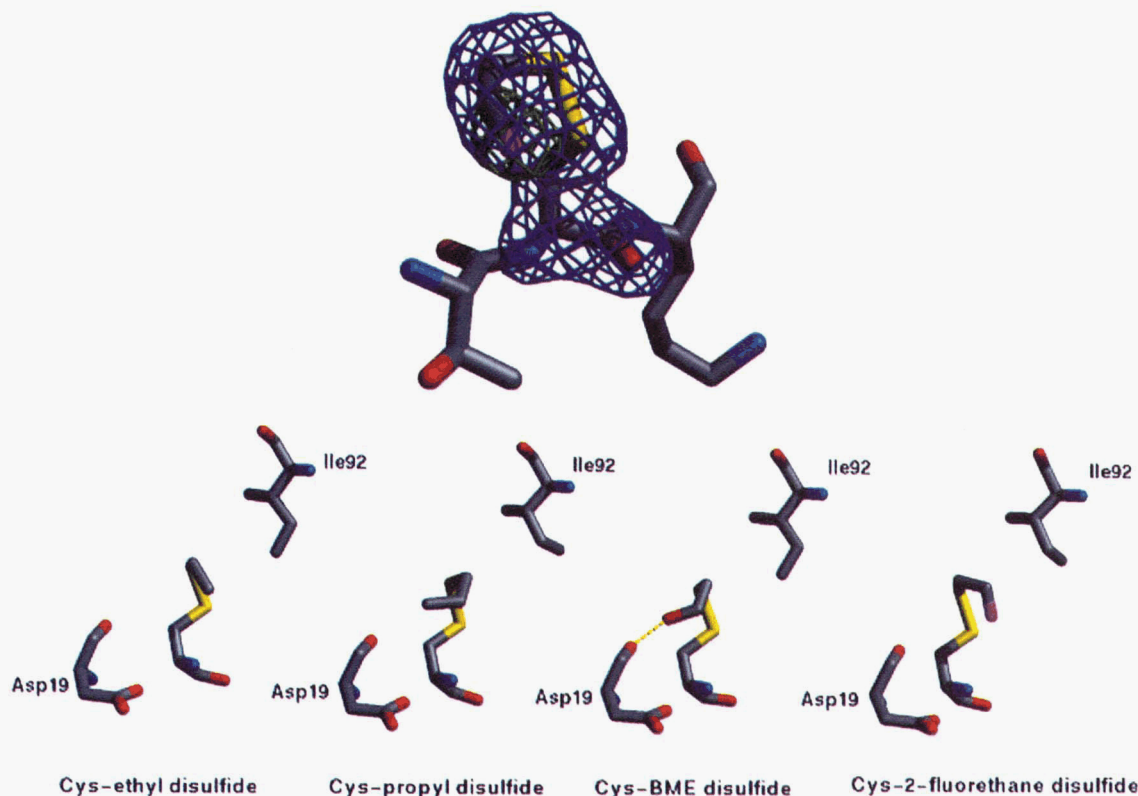


Fig. 3. Top: Fluoroethane variant ($F_o - F_c$) position 23 omit map (blue) and ($F_o - F_c$) fluorine omit map (green). Figure was produced as described in the legend to Figure 2. Bottom: Comparison of ethyl, propyl, BME, and fluoroethane packing. Atoms are color coded according to atom type.

chain carbonyl of residue 19 pulls the BME moiety away from position 92 such that no rotamer change is observed (Fig. 3, bottom panel, right center). The main difference in side conformation between the ethyl variant and the similarly placed propyl and BME variants is a switch in χ_4 (8.0° to -50° or -48°). The fluoroethane variant shows behavior intermediate between all of these. While its side-chain conformation is most similar to the ethyl side chain (see Fig. 3, bottom panel), the Ile92 rotamer change observed in the propyl structure is also observed. Thus, the protein interior apparently discriminates between a proton, fluorine atom, hydroxyl group, or methyl group at this position. This observation is testament to the extreme subtlety of the factors that govern protein folding and binding processes.

Summary

We have shown that introduction of covalent constraints, by cyclization of unnatural amino acids, decreases the thermal motion of these residues in protein interiors. The fact that these side chains populate well known conformations for cyclic hydrocarbons suggests that torsional angle energies strongly influence the behavior of these groups when incorporated into protein interiors and that packing has smaller effects on side-chain conformation and dynamics. The change of a hydrogen atom for a methyl group, hydroxyl group, or fluorine atom shows significant discrimination by the protein core. These results highlight the fine balance of many forces involved in protein–protein interactions.

Materials and methods

Organic synthesis

Proton NMR spectra were taken on a Bruker WM-250 spectrometer. All chemical shifts were relative to tetramethylsilane. Mass spectral analyses were carried out on an HP-5971A mass spectrometer interfaced to an HP-5990 series II gas chromatography system.

2-Fluoroethane methanethiosulfonate was synthesized by mixing 1.0 g 2-fluorobromoethane (7.9 mmole) with 0.65 g sodium

methanethiosulfonate (4.9 mmole) in 15 mL of ethanol and refluxed for 20 h. 100 mL of water was added and the mixture was extracted against three 100 mL portions of CHCl₃. The combined CHCl₃ portions were dried with MgSO₄ and evaporated under reduced pressure. H1 NMR (CDCl₃) δ 4.70 (2H,2T), 3.47 (2H,2T), 3.37 (3H,S). Mass spec. 158(39), 125(13), 79(100). Yield = 0.68 g (89%).

Cyclopentane disulfide was synthesized by mixing 9.55 g of cyclopentane mercaptan (0.093 moles) with 50.0 mL of 15% NaOH. 11.8 g I₂ (0.046 moles) was added with stirring over a period of 30 min. The mixture was stirred overnight, taken up in 100 mL of CHCl₃ and extracted against three 100 mL portions of water. The CHCl₃ layer was dried with MgSO₄ and evaporated under reduced pressure. H1 NMR (CDCl₃) δ 3.29 (1H,M), 1.96 (2H,M), 1.75 (6H,M). Mass spec. 202(36), 134(64), 69(100). Yield = 9.11 g (98%).

Cyclopentyl methanethiosulfonate was synthesized by mixing 1.0 g cyclopentane disulfide (4.9 mmole), 0.86 g AgNO₃ (5.06 mmole), and 0.51 g sodium methanethiosulfonate (5.00 mmole) in 150 mL 50% (v/v) acetone with magnetic stirring. After 15 h, the reaction mixture was filtered and evaporated under reduced pressure. The remaining residue was taken up in 100 mL CHCl₃ and extracted against three 100 portions of water. H1 NMR (CDCl₃) δ 3.73 (1H,M), 3.32 (3H,S), 2.21 (2H,M), 1.68 (6H,M). Mass spec. 180(22), 108(23), 100(73), 67(462). Yield = 0.64 g (73%).

Cyclohexane disulfide was synthesized using the same procedure described above for cyclopentane disulfide. Starting from 9.50 g cyclohexyl mercaptan and 10.37 g I₂, 7.7 g of cyclohexane disulfide (82%) were obtained. H1 NMR (CDCl₃) δ 2.68 (1H,M), 2.05 (2H,M), 1.76 (2H,M), 1.25 (6H,M). Mass spec. 230(25), 148(62), 83(100).

Cyclohexyl methanethiosulfonate was synthesized as described above for cyclopentyl methanethiosulfonate. Starting with 2.0 g cyclohexyl disulfide, 1.41 g cyclohexyl methanethiosulfonate was obtained (84%). H1 NMR (CDCl₃) δ 3.52 (1H,m), 3.31 (3H,S), 2.12 (2H,M), 1.80 (2H,M), 1.52 (6H,M). Mass spec. 194(9.8), 115(13), 114(16), 83(100).

Table 1. X-ray data statistics

	Hexyl	Heptyl	Cyclopentyl	Cyclohexyl	Fluoroethyl
Space group	P41	P41	P41	P41	P41
<i>a</i> = <i>b</i> (Å)	48.1	48.6	48.2	48.6	48.4
<i>c</i> (Å)	63.4	63.2	63.2	62.4	63.3
Resolution range	6.0–2.2	6.0–2.05	6.0–2.20	6.0–2.05	6.0–2.10
No. of unique reflections	5,828	7,032	5,789	7,657	6,874
% Unique reflections	83.1	79.1	82.5	86.9	83.8
High resolution bin	2.29–2.20	2.14–2.05	2.30–2.20	2.14–2.05	2.19–2.10
% complete	71.9	61.7	74.3	72.4	68.8
<i>R</i> -merge ^a	0.064	0.068	0.062	0.059	0.070
Redundancy	4.5	6.0	5.8	6.2	6.4
<i>R</i> -factor ^b	0.164	0.173	0.174	0.169	0.162
No. of water molecules	34	32	34	40	38
Mean <i>B</i> -factor					
Main-chain atoms	35.6	29.3	30.6	34.4	32.0
Side-chain atoms	40.3	33.3	35.2	38.9	36.1

^a*R*-merge = $\sum(\text{Abs}(I - \langle I \rangle))/\sum\langle I \rangle$.

^b*R*-factor = $\sum_{h,k,l} |F_{\text{obs}}(h)| - k|F_c(h)| / |\sum_{h,k,l} F_{\text{obs}}(h)|$.

1-n-hexyl disulfide was synthesized using the same procedure described above for cyclopentane disulfide. Starting from 5.02 g of 1-n-hexane thiol, 4.77 g of product was obtained (95%). H1 NMR (CDCl_3) δ 2.68 (2H,T), 1.64 (2H, M), 1.31 (6H,M), 0.88 (3H,T). Mass spec. 234(100), 150 (83), 117 (70), 85 (73).

1-n-hexyl methanethiosulfonate was synthesized as described above for cyclopentyl methanethiosulfonate. Starting with 1.00 g of 1-n-hexyl disulfide, 0.62 g of product was obtained (74%). H1 NMR (CDCl_3) δ 3.32 (3H,S), 3.18 (2H,T), 1.76 (2H, P), 1.35 (6H,M), 0.88 (3H,T). Mass spec. 117 (92), 83 (100), 55 (92).

1-n-heptyl disulfide was synthesized as described above for cyclopentyl methanethiosulfonate. Starting with 6.03 g of 1-n-heptane thiol, 5.70 g of product was obtained (94%). H1 NMR (CDCl_3) δ 2.69 (2H,T), 2.68 (2H,P), 1.32 (8H,M), 0.89 (3H,T). Mass spec. 262 (55), 164 (37), 131 (37), 57 (100).

1-n-heptyl methanethiosulfonate was synthesized as described above for cyclopentyl methanethiosulfonate. Starting with 1.02 g of 1-n-heptyl disulfide, 0.54 g of product was obtained (66%). H1 NMR (CDCl_3) δ 3.33 (3H,S), 3.18 (2H,T), 1.78 (2H,P), 1.28 (8H,M), 0.88 (3H,T).

Protein chemistry

The nuclease mutants used in this study were produced by a procedure described in Wynn et al. (1995). All structures reported are nuclease- Ca^{2+} -pdTp ternary complexes. Crystallization, data collection, and structure refinement procedures were carried out as in our previous study (Wynn et al., 1996). The data statistics are presented in Table 1. Cavity volumes were calculated using the program GRASP (Nicholls et al., 1993) as previously described (Wynn et al., 1996).

Acknowledgments

We thank Gerry Olack and Patrick Fleming for technical help and helpful discussion. Supported in part by NIH grant GH-51332 to RDF.

References

- Banaszak L, Winter N, Xu Z, Bernlohr DA, Cowan S, Jones TA. 1994. Lipid-binding proteins: A family of fatty acid and retinoid transport proteins. *Adv Prot Chem* 45:89–151.
- Brunger AT. 1992. *X-PLOR Manual, Version 3.0*. New Haven, Connecticut: Yale University.
- Cui W, Li F, Allinger NL. 1993. Simulation of conformational dynamics with the MM3 force field: The pseudorotation of cyclopentane. *J Am Chem Soc* 115:2943–2951.
- Doig AJ, Sternberg MJE. 1995. Side-chain conformational entropy in protein folding. *Protein Sci* 4:2247–2251.
- Fuchs B. 1978. Conformations of five-membered rings. *Topics in Stereochem* V10:1–78.
- Hubbard SJ, Gross K-H, Argos P. 1994. Intramolecular cavities in globular proteins. *Protein Eng* 7:613–626.
- Jacobs MD, Fox RO. 1994. Staphylococcal nuclease folding intermediate characterized by hydrogen exchange and NMR spectroscopy. *Proc Natl Acad Sci USA* 91:449–453.
- Karplus M, Ichiye T, Petit BM. 1987. Configurational entropy of native proteins. *Biophys J* 52:1083–1085.
- Loll PJ, Lattman EE. 1989. The crystal structure of the ternary complex of staphylococcal nuclease, Ca^{2+} , and the inhibitor pDTp, refined at 1.65 Å. *Proteins Struct Funct Genet* 5:183–201.
- Nicholls A, Bharadwaj R, Honig B. 1993. GRASP graphical representation and analysis of surface properties. *Biophys J* 64(2):A166.
- Ponder JW, Richards FM. 1987. Tertiary templates for proteins: Use of packing criteria in the enumeration of allowed sequences for different structural classes. *J Mol Biol* 193:775–791.
- Rance M, Jeffrey KR, Tulloch AP, Butler KW, Smith JC. 1980. Orientational order of unsaturated lipids in the membranes of *Acholeplasma laidlawii* as observed by 2H-NMR. *Biochim Biophys Acta* 600:245–262.
- Richards FM. 1977. Areas, volumes, packing, and protein structures. *Annu Rev Biophys Bioeng* 6:151–176.
- Sacchettini JC, Gordon JL, Banaszak LJ. 1989. Crystal structure of rat intestinal fatty-acid-binding protein. *J Mol Biol* 208:327–339.
- Wand AJ, Urbauer JL, McEvoy RP, Bieber RJ. 1996. Internal dynamics of human ubiquitin revealed by 13C-relaxation studies of randomly fractionally labelled protein. *Biochemistry* 35:6116–6125.
- Wynn R, Richards FM. 1993. Unnatural amino acid packing mutants of *Escherichia coli* thioredoxin produced by combined mutagenesis/chemical modification techniques. *Protein Sci* 2:395–403.
- Wynn R, Anderson CL, Richards FM, Fox RO. 1995. Interactions in non-native and truncated forms of staphylococcal nuclease as indicated by mutational free energy changes. *Protein Sci* 4:1815–1823.
- Wynn R, Harkins P, Richards FM, Fox RO. 1996. Mobile unnatural amino acid side chains in the core of staphylococcal nuclease. *Protein Sci* 5:1026–1031.